

Discrete Wavelets on Edges

Alexandre Chapiro¹, Tassio Knop De Castro¹, Virginia Mota², Eder De Almeida Perez², Marcelo Bernardes Vieira² and Wilhelm Passarella Freire²

¹*Instituto de Matemática Pura e Aplicada,*

²*Universidade Federal de Juiz de Fora
Brazil*

1. Introduction

Human life is closely tied to signals. These signals are present everywhere - listening to music is possible because of audible sound signals traveling through air, reading a book is feasible due to light waves bouncing off objects and interpreted by our bodies as visual images, electromagnetic waves allow us to communicate through the radio or wireless Internet.

Signal Processing is an area of electrical engineering and applied mathematics that deals with either continuous or discrete signals. Particularly, Image Processing is any kind of Signal Processing where the input is an image, such as a digital photograph. The underlying essence of Image Processing lies in understanding the concept of what is an image and studying techniques for the manipulation of images with the use of a computer. While these explanations may seem quite generic, the importance of Image Processing in the modern world is undeniable and progress in this field is very desirable.

1.1 Images

The concept of an image can initially be mathematically defined as a function $f : S \rightarrow C$ that goes from a certain space S (such as \mathbb{R}^2 , for instance) to a space C of colors that can be perceived by the human eye. This definition does not exhaust all of the possible meanings of this word, but will be enough for this chapter. When working on a computer, however, both the domain and counter-domain of the image-function must be discrete. The most common representation of an image in Image Processing thus consists of taking a discrete subset of $S - S'$ and a function that associates the values of S' to a certain subset of $C - C'$. In this way, an image I can be thought of as a discrete function $I : S' \rightarrow C'$.

In this work and in Image Processing in general, the kind of image we are most interested in is a digital image, usually obtained through a digital camera or generated by a computer. As the previous mathematical definition, digital images are discrete, that is they are composed of a finite number of elements. A digital image can be thought of as a mosaic of colors taken from a certain set. In mathematical terms, a digital image can be represented via a matrix $M \in M_{n,m}$, composed of numbers that represent colors that can be shown by modern electronic devices, such as televisions, computer monitors and projectors. Each element of this matrix is called a pixel (this name comes from the words 'picture element').

It is important to understand the concept of color. Initially, color is a sensation produced by the human brain when it receives certain visual stimuli. This input is given by electromagnetic radiation (or light) in a set wavelength that is called the visible spectrum. A typical human eye will respond to wavelengths from about 390 to 750 nm. Theoretically speaking, the space

of all visible colors, as given by their wavelengths is of infinite dimension, and thus not fit for a computer. This limitation is bypassed through the study of the human vision.

Scrutiny of the human eyes shows that they contain two different kinds of photo-receptor cells that allow vision. These cells are rods and cones. Rods are very sensitive to light, being mostly responsible for night vision and have little, if any, role in color vision. Cones on the other hand are of three types (Short, Medium and Long), each covered in a different photo-sensitive pigment. These pigments respond differently to incoming light wavelengths. A chart showing the response of each kind of cone to light can be seen below in Figure 1.

By using the knowledge above, modern visual devices are built so that they emit light at only three different wavelengths, specifically suited to excite each cone in a known way. This allows devices to create a wide range of visible colors. While its not possible to re-create all possible color sensations using only these three colors, the difference when using modern technology is mostly imperceptible. Thus we have arrived at the discretization of the color space used for digital images. These colors can now be codified as certain finite amounts taken in small intervals of these three primary colors. A schematic of a digital image can be seen in Figure 2.

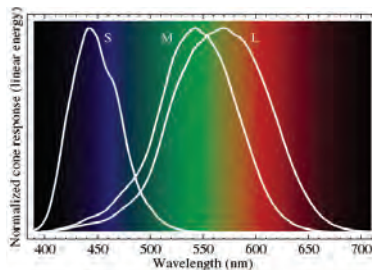


Fig. 1. Human eye response curves. (Image in Public Domain)

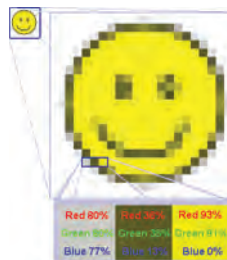


Fig. 2. Raster Image. (Image in Public Domain)

1.2 Applications of Image Processing

Image Processing has seen a great variety of methods developed in the last fifty years. These techniques are greatly diverse and are present in various aspects of human daily life, as well as other important scientific fields.

Some typical tasks in Image Processing involve text or pattern recognition by a computer (machine vision), like identifying individuals from photographs, for instance using their face, retina or fingerprints. In this last case, a specialized camera is used to create a digital image of a person's fingers. This image is then analyzed by a computer program that searches for patterns, which are larger characteristics of the ridges in the skin, and minutia - smaller details

such as ends and bifurcations of said ridges. Figure 3 shows a program extracting information from a finger photograph and Figure 4 shows a fingerprint recognition device being used.

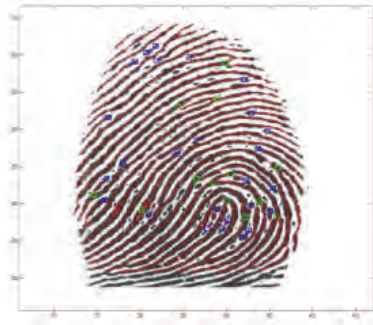


Fig. 3. Human fingerprint analysis. (Image in Public Domain)



Fig. 4. Biometric reading device. (Image in Public Domain)

Other applications involve various methods of obtaining valuable data from several image sources, such as satellites or other sensors in order to discover important characteristics. Several software products such as Photoshop (trademark of Adobe Systems Incorporated) and GIMP (trademark of The GIMP Development Team) rely on common Image-Processing techniques to alter or improve the quality of images. An example of this is High Dynamic Range imaging - a method that blends the information from several differently exposed digital photographs in order to obtain a better view of the scene. An excellent source of information on this topic can be found at (Max Planck Institut fur Informatik, n.d.). See Figure 5 below for an example.

Image Processing can be used to allow cars and other machines to operate automatically by interpreting the information of a video-camera and determining the shapes or movement of objects on the visible scene. An example of a new technology that involves heavy use of Image-Processing in this way is the new Kinect gaming system developed by Microsoft for the Xbox360 console. This device is comprised of three cameras, two of which serve the purpose of analyzing the distance of objects on the scene from the device using an infrared laser. These images are then processed so that the system is able to separate the location of the players from the background or other objects in a process called segmentation (Shotton et al., 2011). An image of this device can be seen on Figure 6. An example of image segmentation can be seen in Figure 7, where the frog is separated from the background.

These and other applications show the importance of Image Processing as a field of research. A good overview of the whole field of Image Processing can be found in (Velho et al., 2008).



Fig. 5. An example of HDR creation from multiple differently-exposed images. (Source exposures by Grzegorz Krawczyk)



Fig. 6. The Kinect gaming device. (Image in Public Domain)



Fig. 7. An example of image segmentation. The frog is being segmented from the background.

Some more information on interesting applications of this field and otherwise can be found in (Acharya & Ray, 2005).

2. A quick glance at wavelet transforms applied to edge detection

The first mention of wavelets appeared in (Haar, 1911). But only in the 1980s did Stephane Mallat (Mallat, 1989) spearheaded the use of wavelets in his work with digital image processing. Inspired by this work, Yves Meyer (Meyer, 1987) constructed the first non-trivial wavelets, which were differentiable, unlike Haar wavelets. They did not, however, have compact support. A few years later, Ingrid Daubechies (Daubechies, 1988) used the works of Mallat to construct a set of orthonormal bases of wavelets with compact support. These works of Daubechies are the foundation of the current use of wavelets in Image Processing. More historical information on wavelets can be found in (Daubechies, 1992).

There are plenty of uses of wavelets in image processing. For example, in 1994 (Fröhlich & Weickert, 1994) presented an algorithm to solve a nonlinear diffusion equation in a wavelet basis. This equation has the property of edge enhancement, an important feature for image processing. More applications in edge detection are shown later in this chapter. The JPEG 2000 image coding system (from the Joint Photographic Experts Group) uses compression techniques based on wavelets. In (Walker, 2003) the author describes a wavelet-based technique for image denoising. Applications of the wavelet transform to detect cracks in frame structures is presented by (Ovanosova & Suárez, 2004). Wavelet transforms have an important role in multiresolution representations in order to effectively analyze the content of images. Multiresolution will be introduced later in this chapter.

2.1 Wavelet Transforms

While the Fourier transform decomposes a signal over sine functions with different frequencies, the wavelet transform decomposes a signal onto translated and dilated versions of a wavelet. Figure 8 shows both a sine wave for the Fourier transform and a wavelet for wavelet transform.



Fig. 8. A sine wave and a wavelet (image from (Radunivić, 2009))

Unlike the Fourier transform, the wavelet transform can capture both frequency and location information.

A wavelet is a function $\psi \in L^2(\mathbb{R})$ with a zero average:

$$\int_{-\infty}^{+\infty} \psi(t) dt = 0 \quad (1)$$

This function is normalized $\|\psi\| = 1$, and centered in the neighborhood of $t = 0$. A family of time-frequency atoms is obtained by scaling ψ by s and translating it by u :

$$\psi_{u,s}(t) = \frac{1}{\sqrt{s}} \psi\left(\frac{t-u}{s}\right) \quad (2)$$

Thus, the Continuous Wavelet Transform (CWT) of a function f at a scale $s > 0$ and translated by $u \in \mathbb{R}$ can be written as:

$$Wf(u,s) = \int_{-\infty}^{+\infty} f(t) \frac{1}{\sqrt{s}} \psi^*\left(\frac{t-u}{s}\right) dt \quad (3)$$

In the field of image processing we are interested in wavelets which form a base of $L^2(\mathbb{R}^2)$ to represent images. If we have an orthonormal wavelet basis in $L^2(\mathbb{R})$ given by ψ with the scaling function ϕ , we can use

$$\begin{aligned} \psi^1(x_1, x_2) &= \phi(x_1)\psi(x_2), \\ \psi^2(x_1, x_2) &= \psi(x_1)\phi(x_2), \\ \psi^3(x_1, x_2) &= \psi(x_1)\psi(x_2), \end{aligned} \quad (4)$$

to form an orthonormal basis in $L^2(\mathbb{R}^2)$ (Mallat, 1999):

$$\left\{ \psi_{j,p}^1, \psi_{j,p}^2, \psi_{j,p}^3 \right\}_{[j,p] \in \mathbb{Z}^3} \tag{5}$$

where ψ^1 corresponds to variations along rows, ψ^2 corresponds to variations along columns and ψ^3 corresponds to variations along diagonals.

It is computationally impossible to analyze a signal using all wavelet coefficients. Thus, for discrete computations, we have to use a Discrete Wavelet Transform (DWT), that is a wavelet transform for which the wavelets are discretely sampled (Mallat, 1999).

Let $f[n] = f(n)$ be the discrete signal of size N . Its discrete wavelet transform is computed at scales $s = a^j$. A discrete wavelet scaled by a^j is defined by:

$$\psi_j[n] = \frac{1}{\sqrt{a^j}} \psi \left(\frac{n}{a^j} \right) \tag{6}$$

The DWT can then be written as a circular convolution $\bar{\psi}_j[n] = \psi_j^*[n]$:

$$Wf(n, a^j) = \sum_{m=0}^{N-1} f[m] \psi_j^*[m-n] = f \star \bar{\psi}_j[n] \tag{7}$$

A wavelet transform computed up to a scale a^J is not a complete signal representation (Mallat, 1999). We need to add the low frequencies $Lf[n, d]$ corresponding to scales larger than d . A discrete and periodic scaling filter is computed by sampling the scaling function $\phi(t)$ defined by:

$$\phi_J[n] = \frac{1}{\sqrt{a^J}} \phi \left(\frac{n}{a^J} \right) \tag{8}$$

Let $\bar{\phi}_j[n] = \phi_j^*[n]$. The low frequencies are carried by:

$$Lf[n, a^J] = \sum_{m=0}^{N-1} f[m] \phi_j^*[m-n] = f \star \bar{\phi}_j[n] \tag{9}$$

As we can see in the Equations 6 and 9, the DWT is a circular convolution. In that way, we will have lowpass and highpass filters which form a bank of filters. Figure 9 shows the discrete wavelet transform for 3 scales. $h_\psi(n)$ is a highpass filter and h_ϕ is a lowpass filter. This form is known as Fast Wavelet Transform (FWT).

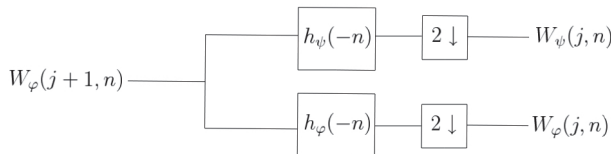


Fig. 9. Fast Wavelet Transform for 1 dimension Mallat (1999)

As we saw before, in the field of image processing we are interested in two dimensional signals. For two dimensions, the DWT of a function $f(x_1, x_2)$ of size $M \times N$ can be written as:

$$\begin{aligned}
 W_\phi(j_0, m, n) &= \frac{1}{\sqrt{MN}} \sum_{x_1=0}^{M-1} \sum_{x_2=0}^{N-1} f(x_1, x_2) \phi_{j_0, m, n}(x_1, x_2) \\
 W_\psi^i(j, m, n) &= \frac{1}{\sqrt{MN}} \sum_{x_1=0}^{M-1} \sum_{x_2=0}^{N-1} f(x_1, x_2) \psi_{j, m, n}^i(x_1, x_2)
 \end{aligned}
 \tag{10}$$

where $i = \{1, 2, 3\}$

Similar to Figure 9, we can express the FWT in two dimensions like the Figure 10.

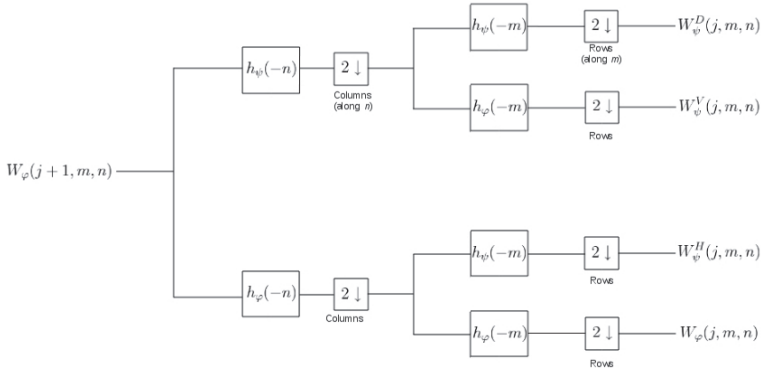


Fig. 10. Fast Wavelet Transform for 2 dimensions Mallat (1999)

For more information on the theory of multiresolution and high-frequency in images, read Section 3.

3. Multiresolution and high frequency in images

Multiresolution Analysis is a very efficient way to process different levels of detail in an image. Detecting and assessing discontinuities of an image allows one to detect its borders, edges and peaks.

3.1 What are high-frequencies?

An image is composed by the sum of its components of low and high frequencies. Low frequencies are responsible for the general smooth areas, while high frequencies are responsible for details, like edges and noise Gonzalez & Woods (2006).

A filter that attenuates high frequencies is called a lowpass filter. A filter that has the opposite characteristic, i.e., highlights high frequencies, is called highpass filter. As we saw on previous sections, in a Discrete Wavelet Transform we have a filter h_ϕ that corresponds a lowpass filter and a filter h_ψ that corresponds a highpass filter.

The Figure 11 shows an example of applying a lowpass filter and a highpass filter on a image. Therefore, high frequencies on images can be used for several applications which need the details of an image, such as detecting edges, corners and textures.

3.2 Multiresolution analysis

A multiresolution analysis of the space $L^2(\mathbb{R})$ consists of a sequence of nested subspaces such that

$$\{0\} \cdots \subset V_0 \subset V_1 \subset \cdots \subset V_n \subset V_{n+1} \subset \cdots \subset L^2(\mathbb{R})$$

with some important properties. The most important characteristics that we consider in the context of image processing for high frequency assessment are:



Fig. 11. Results of lowpass and highpass filters. The first image is the original, the second is the result of a lowpass filter and the third is the result of a highpass filter

- **Regularity**
The subspace V_0 is generated as the linear combination of integer shifts of one or a finite number of generating functions ϕ_1, \dots, ϕ_r . These generating functions are called scaling functions. Usually those functions must have compact support and be piecewise continuous.
- **Completeness**
those nested subspaces fill the whole space $L^2(\mathbb{R})$, and they are not too redundant. So, the intersection of these subspaces should only contain the zero element.

This concept, applied to image processing and wavelets, justifies the successful use of image pyramids in the context of high frequency detection.

3.3 Image pyramids

A simple, but powerful, structure to represent images at more than one resolution is the image pyramid Burt & Adelson (1983). Basically, it is a collection of decreasing resolution images arranged in the shape of a pyramid (Figure 12).

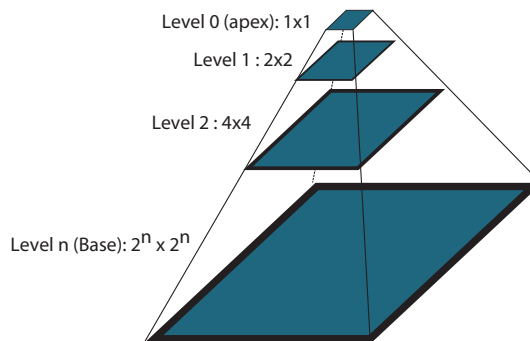


Fig. 12. Image Pyramid.

The idea behind image pyramids is to generate a number of images corresponding to the response of a bank of filters at different scales. There are many different types of filters that can be used for this purpose.

One special family of filters consists of Wavelets. They are constructed from a mother wavelet. A family is constructed by dilating and translating the mother wavelet by different quantities. The main advantage of using this family of functions over the Fourier transform is that wavelets respond very well to discontinuities, i.e, high frequencies. The most know wavelet families are the Haar, Daubechies, Coiflet, and Symmlet.

The Daubechies family is of particular interest because it is fractal in nature, and the Haar family, although very simple, can be very useful in many applications.

In practical terms, the base of the pyramid is the image which we want to filter in various scales, and each level of the pyramid above the base is produced by filtering it and generating an image with half of its width and height.

Using wavelet and scale functions, the nested subspaces of scale and detail are produced. The horizontal, vertical and diagonal details of a subspace V_{i+1} are the information that cannot be represented in V_i (Figure 13).

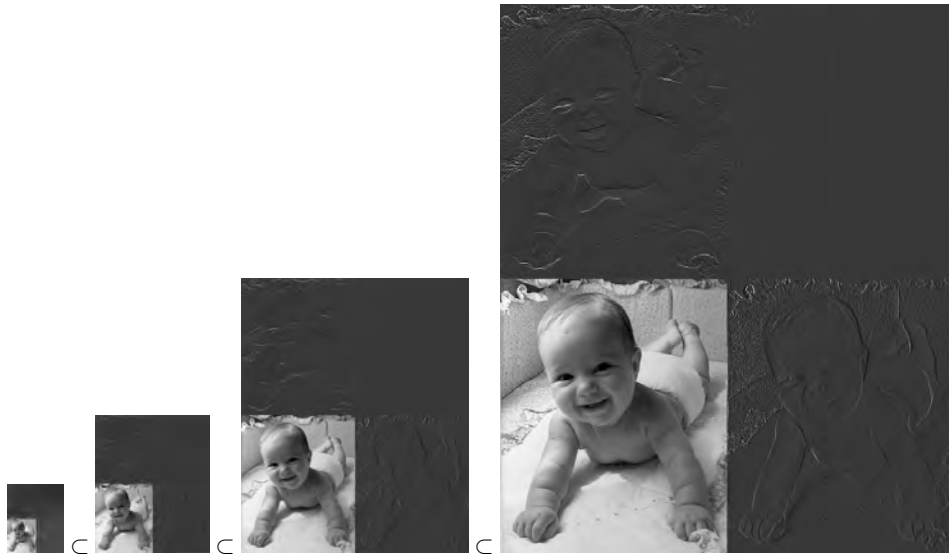


Fig. 13. Nested subspaces in the context of image processing. The details are represented in the grey regions (the contrast was enhanced for better visualization).

Now is easy to understand how the discrete wavelet transform can be applied for images. As we saw in Equation 10, the Discrete Wavelet Transform in two dimensions captures the variations on rows, columns and diagonals. Figure 14 shows an example of a DWT applied for an image in 3 scales.

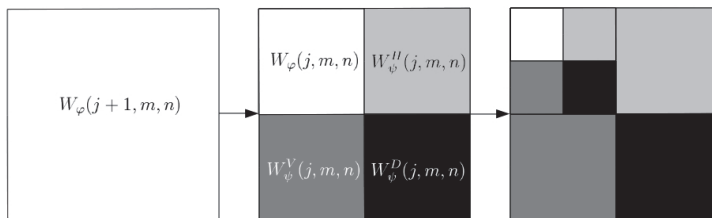


Fig. 14. The result decomposition of a blank image using a discrete Wavelet Transform for 1 and 2 scales Gonzalez & Woods (2006)

Section 4.2 describes a method which produces a pyramid of a chosen image and processes the correspondent details in every scale. This allows us to detect discontinuities in a very precise and adaptative approach.

3.4 Edge detectors using multiresolution and discrete wavelet transform

Many works use multiresolution as a step to gather specific image information on a single scale. The idea is to combine the information present at several scales, as appearance is related to the scale of the observation, so a scene should be described at multiple scales.

The first ones to formalize this concept were Witkin (1983) and Koenderink (1984) with the idea of scale-space linear filtering. The principle is to convolve the original image by a family of Gaussians of increasing variance related to the studied scale, and then to progressively eliminate the smallest structures in the image.

However, this approach suffers from several drawbacks such as blurred edges and the edges at the coarse scale are shifted. Multiple nonlinear diffusion filters have been suggested to overcome these drawbacks. More elaborated approaches have been suggested to accelerate the resolution, such as wavelet-based ones.

Recent works still use the idea of convolution by a family of Gaussians (Sumengen & Manjunath (2005), Zhang et al. (2010)) and nonlinear diffusion filters (Tremblais & Augereau (2004)). Other works are wavelet-based, as can be seen in (Belkasim et al., 2007), (Shih & Tseng, 2005), (Han & Shi, 2007), Brannock & Weeks (2006) and Heric & Zazula (2007).

Sumengen & Manjunath (2005) create an Edgeflow vector field where the vector flow is oriented towards the borders at either side of the boundary. To create this vector field, they use a fine to coarse strategy. In that way, the proposed method favors edges that exist at multiple scales and suppress edges that only exist at finer scales. The strength of the edges are represented by the strength of the vectors at the edge location where the vector field changes its direction. This method is also used to multi-scale image segmentation.

Tremblais & Augereau (2004) present a new explicit scheme to the linear diffusion filtering which preserves edges. A fast filtering algorithm is then combined with a simple multiscale edge detection algorithm.

For Zhang et al. (2010), the one pixel width edge is more accurate than other edge detection. So, they explore the zero-crossing edge detection method based on the scale-space theory.

For image segmentation, Belkasim (Belkasim et al., 2007) uses a wavelet-based image analysis scheme based on extracting all objects in the image using their borders or contours. The size of the contour can then be used to define the level of resolution and hence the extent of the analysis.

Shih (Shih & Tseng, 2005) argue that edge extraction based only on a gradient image will produce a bad result with noise and broken edges. In order to solve this problem, they combine an edge detector with a multiscale edge tracker based on the discrete wavelet transform.

In Han (Han & Shi, 2007), the wavelet transform plays an important role in the task of decomposing a texture image into several levels. Once a decomposition level is chosen, textures are then removed from the original image by the reconstruction of low frequencies only.

The problem for Brannock & Weeks (2006) is to automatically detect edges. To determine its efficacy, the 2D discrete wavelet transform is compared to other common edge detection methods. They conclude that the discrete wavelet transform is a very successful edge-detection technique, especially when utilizing auto-correlation.

Heric & Zazula (2007) present a novel edge detector based on the wavelet transform and signal registration. The proposed method provides an edge image by a time-scale plane based edge detection using a Haar wavelet. Then, this edge image is used in a registration procedure in order to close the edge discontinuities and calculate a confidence index for the detected contour points.

4. The DWT applied to high-frequency assessment from multiresolution analysis

In this section, we present a practical use of wavelets for visualization of high frequency regions of a multiresolution image. Our approach combines both multiresolution analysis and orientation tensor to give a scalar field representing multiresolution edges. Local maxima of this scalar space indicate regions having coincident detail vectors in multiple scales of wavelet decomposition. This is useful for finding edges, textures, collinear structures and salient regions for computer vision methods. The image is decomposed into several scales using the DWT. The resulting detail spaces form vectors indicating intensity variations which are adequately combined using orientation tensors. A high frequency scalar descriptor is then obtained from the resulting tensor for each original image pixel.

4.1 Orientation tensor

One way of estimating salient regions in image processing is to use multiresolution to capture global and local brightness variations. Even in a non-redundant wavelet decomposition, local and global borders occurring in the same region may carry useful information. The problem lies in combining this global information into a single image. In this way, we can capture the multivariate information of several scales and color channels using orientation tensors (Knutsson, 1989).

A local orientation tensor is a special case of non-negative symmetric rank 2 tensor, built based on information gathered from an image. As shown by Knutsson (Knutsson, 1989), one can be produced by combining outputs from polar separable quadrature filters. Because of its construction, such a tensor has special properties and contains valuable information about said image.

From definition given by Westin (Westin, 1994), orientation tensors are symmetric, and thus an orientation tensor T can be decomposed using the Spectral Theorem as shown in Equation 11, where λ_i are the eigenvalues of T .

$$T = \sum_{i=1}^n \lambda_i T_i \tag{11}$$

If T_i projects onto a m -dimensional eigenspace, we may decompose it as

$$T_i = \sum_{s=1}^m e_s e_s^T \tag{12}$$

where $\{e_1, \dots, e_m\}$ is a base of \mathbb{R}^m . An interesting decomposition of the orientation tensor T (Westin, 1994) is given by

$$T = \lambda_n T_n + \sum_{i=1}^{n-1} (\lambda_i - \lambda_{i+1}) T_i \tag{13}$$

where λ_i are the eigenvalues corresponding to each eigenvector e_i . This is an interesting decomposition because of its geometric interpretation. In fact, in \mathbb{R}^3 , an orientation tensor T decomposed using Equation 13 can be represented by a spear (its main orientation), a plate and a ball

$$T = (\lambda_1 - \lambda_2) T_1 + (\lambda_2 - \lambda_3) T_2 + \lambda_3 T_3 \tag{14}$$

A \mathbb{R}^3 tensor decomposed by Equation 14, with eigenvalues $\lambda_1 \geq \lambda_2 \geq \lambda_3$, can be interpreted as following:

- $\lambda_1 \gg \lambda_2 \approx \lambda_3$ corresponds to an approximately linear tensor, with the spear component being dominant.

- $\lambda_1 \approx \lambda_2 \gg \lambda_3$ corresponds to an approximately planar tensor, with the plate component being dominant.
- $\lambda_1 \approx \lambda_2 \approx \lambda_3$ corresponds to an approximately isotropic tensor, with the ball component being dominant, and no main orientation present

Consider two orientation tensors A and B and its summation $T = A + B$. After the decomposition of T using Equation 14, the component $(\lambda_1 - \lambda_2)T_1$ is an estimate of the collinearity of the main eigenvectors of A and B .

4.2 Proposed method

The method proposed in (de Castro et al., 2009) uses high frequency information extracted from wavelet analysis. Given an input image I , for each scale j and position $p \in I$, we create a vector $v_{j,p}$ as follow:

$$v_{j,p} = [I \cdot \psi_{j,p}^1, I \cdot \psi_{j,p}^2, I \cdot \psi_{j,p}^3]^T \quad (15)$$

This vector contains the high frequency value at vertical, horizontal and diagonal directions of the image I at the position p and scale j . Simmetric rank 2 tensors are then created as

$$M_{j,p} = v_{j,p} v_{j,p}^T \quad (16)$$

We find the final tensor $M_{0,p}$ for each pixel of the original image using

$$M_{0,p} = \sum_{j=1}^{n_j} k_j M_{j,p} \quad (17)$$

to combine the tensors obtained at each scale j , where n_j is the number of scales and $k_j \in \mathbb{R}$ is the weight assigned to each scale, given by

$$k_j = \frac{\sum_{n=1}^{n_p} \text{Trace}(M_{j,n})}{\sum_{k=1}^{n_j} \sum_{n=1}^{n_p} \text{Trace}(M_{k,n})} \quad (18)$$

where n_p is the number of pixels and $\text{Trace}(M_{j,p})$ is the sum of the eigenvalues of $M_{j,p}$. The trace represents the amplification driven by the tensor to the unit sphere and is a good estimator of its importance. Thus, the tensor sum is weighted by the proportion of energy of each scale in the multiresolution pyramid.

In order to find $M_{j,p}$ in Equation 17, we use bilinear interpolation of the tensor values, relative to each position p in the initial image, at the subsampled image at scale j to find the resulting tensor $M_{j,p}$ for each pixel of the initial image. This is depicted in Figure 15, where tensors are represented as superquadric glyphs whose longer axis shows the main direction.

Note that the tensor presented in Equation 17 is a 3×3 positive symmetric matrix with real coefficients, and thus we may apply Equation 14. We then find the main orientation component (spear) of the final orientation tensor for each pixel of the input image. This component indicates the collinearity of the interpolated tensors and provides interesting results.

4.2.1 Implementation

The proposed algorithm consists of three main steps: a discrete wavelet transform (Barnard, 1994; Mallat, 1999), a tensor field computation and a weighted sum of the computed tensors. The whole process is illustrated in Figure 16.

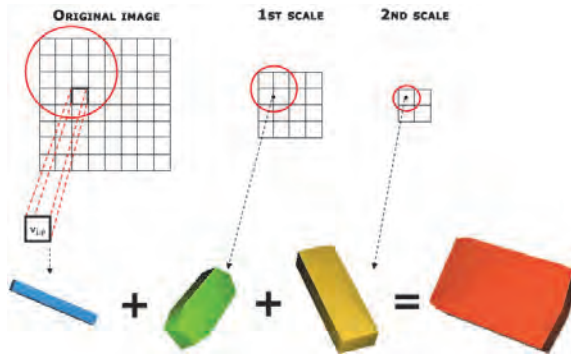


Fig. 15. A tensor is computed for each pixel in original image by a weighted sum of corresponding tensors in each scale. In this example, two wavelet decompositions are performed.

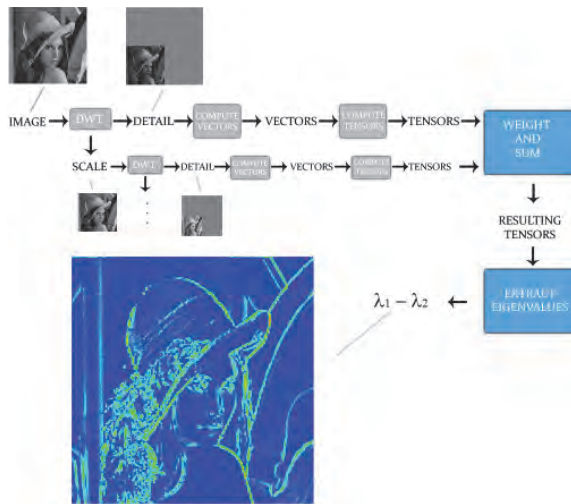


Fig. 16. Example of the proposed algorithm using Daubechies1 to decompose the image into two scales.

The number of scales to be used is a parameter of the algorithm. The DWT splits the image into three detail components and one scale component in the beginning of each iteration. In the next iteration, the same process is applied, using the resulting scale component as the input image.

For each pixel of the input image, its correspondent position at the current scale is computed with subpixel precision for each resolution. The four nearest pixels in a given resolution are used to compute the final tensor. The vectors $v_{j,p}$ described in Equation 15 are computed for each of these pixels and then used to compute four spear type tensors. The final tensor for the subpixel position is obtained by combining these four tensors with bilinear interpolation. The pixel tensor is computed by combining the n_j tensors as showed in Equation 17.

The pixel tensors are decomposed and their eigenvalues are then extracted. The values $\lambda_1 - \lambda_2$ are computed and normalized to form the output image. Color images are split

into three monochromatic channels (Red, Green and Blue) and the proposed algorithm is applied to each channel separately. The tensors for each color channel are summed before eigen decomposition.

The complexity of the whole process is $O(n_j \cdot n_p)$, where n_j is the number of analyzed scales and n_p the amount of input pixels. Thus, this is an efficient method that can be further parallelized.

4.2.2 Experimental results

The proposed method was tested with several images and using several wavelets functions (de Castro et al., 2009). A piece of the experiments is shown in Figure 17. The DWT is applied with different analyzing Daubechies filters and number of scales. The Church's ceiling is formed by coincident frequencies on its geometric details. These details can be better observed in Figure 17c.

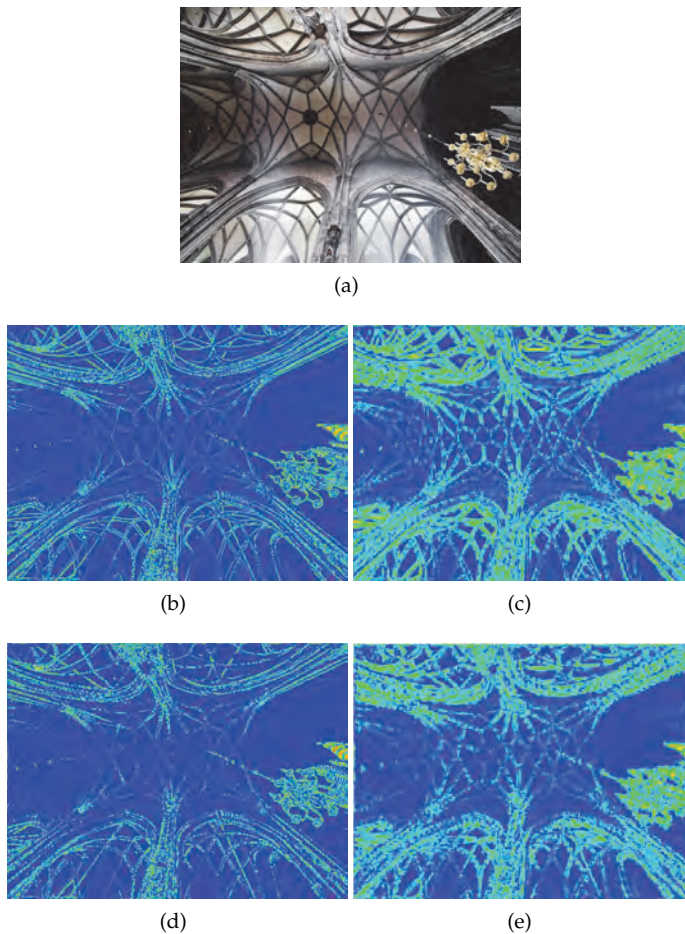


Fig. 17. (a) input image. (b) $\lambda_1 - \lambda_2$ with Daubechies1 and 1 scale. (c) Daubechies1 and 3 scales. (d) Daubechies3 and 1 scale. (e) Daubechies3 and 3 scales.

A better estimation of soft edge transitions is obtained by changing the analyzing filter from Daubechies1 to Daubechies3. Figures 17b and 17d illustrate this behavior.

In general, it can be noted that this method highlights high frequencies occurring in the same region at different scales. We used thermal coloring with smooth transition from blue to red, where blue means absence of high frequencies, and red means presence of high frequencies. The green regions also indicate high frequencies, but less intense than those indicated by red regions. The red regions provide the better higher frequencies estimation tensors.

4.2.3 Conclusion

We presented an overview of discrete wavelets and multiresolution applied to edge detection. We also presented a method for high frequency assessment visualization using these powerful tools. The method is based on the DWT decomposition and detail information merging using orientation tensors. This multiresolution analysis showed to be suitable for detecting edges and salient areas in an image. The experimental results show that the high frequency information can be inferred by varying the DWT filters and number of scales. Coincident frequencies in space domain are successfully highlighted. By tuning the number of scales, one may infer texture feature regions. The $\lambda_1 - \lambda_2$ scalar field is one of the most used orientation alignment descriptors. However, other relations can be extracted from final tensors. This method can be easily parallelized, the use of technologies like GPGPUs and multicore CPUs turns it attractive for high performance applications.

5. References

- Acharya, T. & Ray, A. K. (2005). *Image Processing - Principles and Applications, First Edition*, Wiley InterScience.
- Barnard, H. J. (1994). *Image and Video Coding Using a Wavelet Decomposition*, PhD thesis, Delft University of Technology, Department of Electrical Engineering, Information Theory Group, P.O.Box 5031, 2600 GA, Delft.
- Belkasim, S., Derado, G., Aznita, R., Gilbert, E. & O'Connell, H. (2007). Multi-resolution border segmentation for measuring spatial heterogeneity of mixed population biofilm bacteria, *Computerized Medical Imaging and Graphics* 32.
- Brannock, E. & Weeks, M. (2006). Edge detection using wavelets, *Proceedings of the 44th annual Southeast regional conference, ACM-SE 44*, ACM, New York, NY, USA, pp. 649–654.
- Burt, P. J. & Adelson, E. H. (1983). The laplacian pyramid as a compact image code, *IEEE Transactions on Communications* 31: 532–540.
- Daubechies, I. (1988). Orthonormal bases of compactly supported wavelets, *Communications on Pure and Applied Mathematics* 41(7): 909–996.
- Daubechies, I. (1992). *Ten lectures on wavelets*, Society for Industrial and Applied Mathematics, Philadelphia, PA, USA.
- de Castro, T. K., de A. Perez, E., Mota, V. F., Chapiro, A., Vieira, M. B. & Freire, W. P. (2009). High frequency assessment from multiresolution analysis., *ICCS (1)*, Vol. 5544 of *Lecture Notes in Computer Science*, Springer, pp. 429–438.
- Fröhlich, J. & Weickert, J. (1994). Image processing using a wavelet algorithm for nonlinear diffusion.
- Gonzalez, R. C. & Woods, R. E. (2006). *Digital Image Processing (3rd Edition)*, Prentice-Hall, Inc., Upper Saddle River, NJ, USA.
- Haar, A. (1911). Zur theorie der orthogonalen funktionensysteme, *Mathematische Annalen* 71: 38–53. 10.1007/BF01456927.
- Han, Y. & Shi, P. (2007). An adaptive level-selecting wavelet transform for texture defect detection, *Image Vision Comput.* 25(8): 1239–1248.

- Heric, D. & Zazula, D. (2007). Combined edge detection using wavelet transform and signal registration, *Image Vision Comput.* 25: 652–662.
- Knutsson, H. (1989). Representing local structure using tensors, *The 6th Scandinavian Conference on Image Analysis*, Oulu, Finland, pp. 244–251. Report LiTH-ISY-I-1019, Computer Vision Laboratory, Linköping University, Sweden, 1989.
- Koenderink, J. J. (1984). The structure of images, *Biological Cybernetics* 50(5): 363–370–370.
- Mallat, S. (1999). *A Wavelet Tour of Signal Processing, Second Edition (Wavelet Analysis & Its Applications)*, Academic Press.
- Mallat, S. G. (1989). A theory for multiresolution signal decomposition: the wavelet representation, *IEEE Transactions on Pattern Analysis and Machine Intelligence* 11: 674–693.
- Max Planck Institut für Informatik, M. (n.d.). <http://www.mpi-inf.mpg.de/resources/hdr/>.
- Meyer, Y. (1987). Principe d'incertitude, bases hilbertiennes et algèbres d'opérateurs. (The uncertainty principle, Hilbert base and operator algebras). Sémin. Bourbaki, 38ème année, Vol. 1985/86, Exp. Astérisque 145/146, 209–223 (1987).
- Ovanesova, A. V. & Suárez, L. E. (2004). Applications of wavelet transforms to damage detection in frame structures, *Engineering Structures* 26(1): 39 – 49.
- Radunović, D. (2009). *WAVELETS from MATH to PRACTICE*, Springer.
- Shih, M. & Tseng, D. (2005). A wavelet-based multiresolution edge detection and tracking, *IVC* 23(4): 441–451.
- Shotton, J., Fitzgibbon, A., Cook, M., Sharp, T., Finocchio, M., Moore, R., Kipman, A. & Blake, A. (2011). Real-time human pose recognition in parts from a single depth image.
- Sumengen, B. & Manjunath, B. S. (2005). Multi-scale edge detection and image segmentation, *European Signal Processing Conference (EUSIPCO)*.
- Tremblais, B. & Augereau, B. (2004). A fast multi-scale edge detection algorithm, *Pattern Recogn. Lett.* 25: 603–618.
- Velho, L., Frery, A. & Gomes, J. (2008). *Image Processing for Computer Graphics and Vision, First Edition*, Springer.
- Walker, J. S. (2003). Tree-adapted wavelet shrinkage, Vol. 124 of *Advances in Imaging and Electron Physics*, Elsevier, pp. 343 – 394.
- Westin, C.-F. (1994). *A Tensor Framework for Multidimensional Signal Processing*, PhD thesis, Department of Electrical Engineering Linköping University.
- Witkin, A. P. (1983). Scale-Space Filtering., *8th Int. Joint Conf. Artificial Intelligence*, Vol. 2, Karlsruhe, pp. 1019–1022.
- Zhang, M., Li, X., Yang, Z. & Yang, Y. (2010). A novel zero-crossing edge detection method based on multi-scale space theory, *Signal Processing (ICSP), 2010 IEEE 10th International Conference on*, pp. 1036–1039.